

Strategies for Efficient Numerical Implementation of Hybrid Multi-scale Agent-Based Models to Describe Biological Systems

NICHOLAS A. CILFONE,¹ DENISE E. KIRSCHNER,² and JENNIFER J. LINDERMAN¹

¹Department of Chemical Engineering, University of Michigan, 3074 H.H. Dow, 2300 Hayward St., Ann Arbor, MI 48109, USA; and ²Department of Microbiology and Immunology, University of Michigan Medical School, Ann Arbor, MI, USA

(Received 12 June 2014; accepted 18 October 2014; published online 8 November 2014)

Associate Editor Michael R. King oversaw the review of this article.

Abstract—Biologically related processes operate across multiple spatiotemporal scales. For computational modeling methodologies to mimic this biological complexity, individual scale models must be linked in ways that allow for dynamic exchange of information across scales. A powerful methodology is to combine a discrete modeling approach, agent-based models (ABMs), with continuum models to form hybrid models. Hybrid multi-scale ABMs have been used to simulate emergent responses of biological systems. Here, we review two aspects of hybrid multi-scale ABMs: linking individual scale models and efficiently solving the resulting model. We discuss the computational choices associated with aspects of linking individual scale models while simultaneously maintaining model tractability. We demonstrate implementations of existing numerical methods in the context of hybrid multi-scale ABMs. Using an example model describing *Mycobacterium tuberculosis* infection, we show relative computational speeds of various combinations of numerical methods. Efficient linking and solution of hybrid multi-scale ABMs is key to model portability, modularity, and their use in understanding biological phenomena at a systems level.

Keywords—Multi-scale modeling, Hybrid modeling, Agent-based modeling, Numerical implementation, Linking models, Tuneable resolution.

INTRODUCTION

Computational models are used in systems biology for understanding, predicting, and translating a wealth of experimentally generated data into a realization of systems behavior. Multi-scale computational models in particular have provided valuable insights for applica-

tion to areas as diverse as infectious disease,^{18,26,27} inflammation,³ cancer,^{24,83,90} angiogenesis,⁶⁷ and disease treatment.^{38,44,58,87} A defining feature of multi-scale computational models is a description of biological mechanisms that operate over different spatiotemporal scales.^{4,76,77,87,89} When building multi-scale models four different areas must be considered (Fig. 1): (1) *constructing* models—how to create a mathematical formulation that is able to recapitulate the dynamics of a biological system at an individual scale, (2) *linking* models—how to join individual scale models to allow for exchange of information, (3) *solving* models—determining the most efficient way to solve the underlying mathematics, and (4) *analyzing* models—how to calibrate and validate the model and then make and understand model predictions. In this paper, we review strategies to link individual scale models and methods to efficiently solve the resulting multi-scale model.

We typically link descriptions of biological phenomena operating at an individual scale together to form a multi-scale model.^{48,87} One approach to linking individual scale models, referred to as hierarchical linking, is to solve the lowest scale (i.e., the smallest length or time scale) model to completion and subsequently feed the output, for example in the form of an initial condition or parameter value, to the model at the next higher scale.^{20,48,87} However, this type of linking methodology is inappropriate when information across scales needs to be continually exchanged and in both directions. For instance, vascular endothelial growth factor (VEGF) can induce an endothelial cell to divide which may elongate a blood vessel in a new direction. The new endothelial cells will produce more VEGF, leading to cellular movement and continued growth of the blood vessel in the new direction.^{67,68} Without exchange of information in both directions (molecular to cellular and cellular to

Address correspondence to Jennifer J. Linderman, Department of Chemical Engineering, University of Michigan, 3074 H.H. Dow, 2300 Hayward St., Ann Arbor, MI 48109, USA. Electronic mail: linderman@umich.edu

molecular), sprouting of new blood vessels would likely not occur. The nature of biological systems, with constant exchange of information across scales, necessitates multi-scale models that mimic this dynamic exchange of information. The resulting multi-scale model is more complex than the individual-scale parts, making it more difficult to link, solve, and analyze than traditional mathematical or computational models. Therefore, efficient strategies and approaches that balance model complexity, computational time, and ease of implementation to link and solve multi-scale models are necessary.

Agent-based models (ABMs, sometimes called individual based models—IBMs) are stochastic, discrete models that utilize individual entities known as *agents*, here representing individual biological cells (Fig. 2). Each agent is autonomous and behaves based on decisions from the set of rules, interactions, and states given to it, leading to heterogeneity between agents. ABMs can generate complex system-level emergent behavior from simple rule-based descriptions of each individual.^{3,11,71,74,87,89} Agents can receive inputs from the environment, influencing their decision making, and can also have the ability to alter their environment. Models that combine aspects of both continuous and discrete model constructs are commonly referred to as *hybrid* models. Hybrid ABMs arise when continuum models are used to describe part of the overall system, such as the environment and parts of the agent decision-making processes.^{4,18,26,38,50,89} A hybrid ABM is also termed multi-scale when a portion of the model, such as the continuum models, describes behaviors occurring at a different spatiotemporal scale than that of the ABM.

We focus this review on providing strategies, guidelines, and a general framework for developing hybrid multi-scale ABMs where an ABM (discrete), is informed by differential equation models (continuous) operating

at a different scale. This review can function as a guide for new modeling efforts (e.g., How are individual scale models be linked? What solution methods should I consider?) and also as a framework for extending existing ABMs into hybrid multi-scale ABMs (e.g., What needs to be incorporated into the existing model? What is the easiest way to get it working?).

We focus on the use of continuum models to describe the dynamics of the environment and agent-associated reactions that occur at a smaller spatial and faster time scale and influence agent decision-making processes (Figs. 2 and 3). These hybrid multi-scale ABMs use a temporally separated approach in which the continuum models are solved using conventional numerical methods on a faster time scale than the ABM; syncing between scales is required to reconcile information exchange.^{22,86} While many platforms exist for developing ABMs (e.g., NetLogo, Repast, Swarm, SPARK, CHASTE, MASON, and FLAME^{5,8,18,22,29,46,73}), we have found the flexibility of an in-house platform (written in an object-oriented programming language C++) necessary to link and solve hybrid multi-scale ABMs. After introducing key modeling concepts, we review how to link individual scale ABMs to differential equation models and efficient implementations of numerical solvers that allow frequent exchange of information across models. Finally, we present a case study in order to demonstrate the trade-off between computational speeds and model complexity using an established hybrid multi-scale ABM of *Mycobacterium tuberculosis* infection.

EXAMPLES OF HYBRID MULTI-SCALE ABMS

Hybrid multi-scale ABMs (Fig. 2) are being used to describe many biological systems. To orient the reader, we briefly review three such systems: epithelial

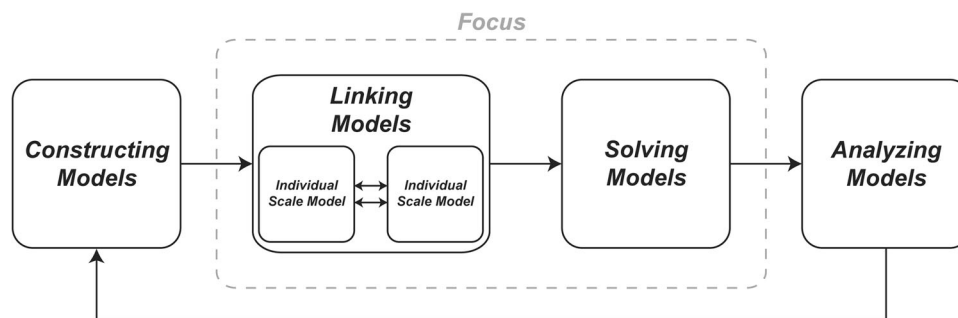


FIGURE 1. Considerations for building multi-scale models. (1) **Constructing models:** how to create mathematical formulations that accurately represent individual scale dynamics of a biological system, (2) **Linking models:** how to connect mathematical formulations of individual scale models to create multi-scale models, (3) **Solving models:** implementing efficient methods to solve multi-scale models, and (4) **Analyzing models:** Understanding and translating model predictions. Model analysis commonly iterates back to model construction in order to include new biological mechanisms of interest/relevance. In this work, we focus on how to link individual scale models and efficiently solve the resultant multi-scale model.

restitution, growth of brain tumors, and immune responses to bacterial pathogens.

Epithelial Restitution

The wound healing response of damaged epithelial cells involves restitution (resealing the epithelial layer), proliferation, and differentiation.⁷⁹ The cytokines transforming-growth-factor- β (TGF- β) and epidermal growth factor (EGF) are necessary for beginning restitution processes, diffusing through the extracellular matrix (Fig. 2c), binding to TGF- β and EGF receptors on endothelial cells, and signaling through SMAD and ERK pathways (Fig. 2b).⁷⁹ In the ABM, endothelial cells are represented as individual agents (Fig. 2a) whose behavior, such as migration and adherence, depends on SMAD and ERK signaling (Fig. 3). At the tissue scale, the reconnection of damaged epithelium (restitution) with healthy endothelial is critical to wound healing and constitutes much of the early wound healing response to damaged tissue. This hybrid multi-scale ABM qualitatively matches temporal experimental data and predicts the importance of environmental interactions on the dynamics of epithelial restitution.

Growth Patterns of Brain Tumors

The expression of EGF receptors in brain tumors is associated with rapid growth and invasion. Yet, in growing tumors, cells only display a single phenotype of either migration or proliferation. Transforming-growth-factor- α (TGF- α) diffuses within the extracellular environment (Fig. 2c) and binds and dimerizes with EGF receptors, initiating downstream signaling through PLC γ (Fig. 2b). These downstream signaling processes mediate the phenotype of a tumor cell (Fig. 3). In the ABM, tumor cells are represented as individual agents (Fig. 2a) with both proliferative and migratory potentials determined by levels of PLC γ and bound EGFR (Fig. 3). The proliferative and migratory nature of tumor cells leads to tumor growth and expansion.^{6,7,88} These hybrid multi-scale ABMs of tumor growth have shown that increased EGF receptor density correlates with tumor expansion based on early phenotypic switching driven by TGF- α autocrine signaling.^{6,7,88}

Immune Response to *Mycobacterium tuberculosis*

During *M. tuberculosis* infection the immune system relies on a variety of cells and molecules to coordinate an effective immune response.^{18,26,28,30,57,71} Two extracellular diffusing molecules of interest are the pro-inflammatory cytokine tumor necrosis factor- α (TNF- α) and the anti-inflammatory cytokine interleukin-10 (IL-10). These cytokines diffuse through the lung tissue

(Fig. 2c), bind to cell-associated receptors (TNFR1, TNFR2, and IL-10R), and signal through pathways such as NF κ B and STAT3 (Fig. 2b). Macrophages and T cells are key immune cells, modeled as agents (Fig. 2a), with many states (e.g., resting, activated, deactivated) and functions (e.g., bactericidal ability) driven by levels of NF κ B and STAT3 (Fig. 3). Control of infection relies on the formation of an organized structure of immune cells, known as a granuloma, and its function over the long timescale of infection. Hybrid multi-scale ABMs of *M. tuberculosis* infection are able to reproduce the emergent phenomenon of granuloma formation and demonstrate a critical balance between TNF- α and IL-10 in controlling granuloma function.^{18,26,28} In addition, the effects of two first-line antibiotics, rifampicin (RIF) and isoniazid (INH), on bacterial burden have been simulated in a hybrid multi-scale ABM.⁶⁴ Antibiotics diffuse through the lung environment (Fig. 2c), are taken up by immune cells (Fig. 2a), and are able to kill bacteria. We use this hybrid multi-scale ABM describing *M. tuberculosis* infection as a case study in a later section to illustrate the principles and numerical methods described in this review.

CENTRAL CONCEPTS FOR HYBRID MULTI-SCALE ABMS

Mathematical Framework and Linking

We describe the elements of a 2-dimensional hybrid multi-scale ABM (Fig. 2), but the methodology presented is easily adapted to any dimensionality required. An ABM describes relevant biological cells (or any unit) as individual agents. Each agent (A) has an associated state (V) and position (x, y) that can change with time. Examples of cell agent states include activated, proliferating, infected, and cancerous. Changes in state are based on a set of stochastic agent rules and interactions, and are also influenced by extracellular diffusing molecules in the environment (e.g., ligands that bind to surface receptors on the cell). The construction of an ABM is beyond the scope of this article but is well-described in the literature.^{1,11,17,29,36,68,70,73,74,79} The concept of agents in an ABM is naturally analogous to objects in an object-oriented programming language, and therefore constructing hybrid multi-scale ABM in a language such as C++ or Java is a logical choice.

For each individual agent, a set of agent-associated reactions can occur:

$$\text{For each } A(x, y, V) : \frac{dY_r}{dt} = f_r(L, Y_1, Y_2, \dots, Y_R, \beta)$$

$$r = 1, 2, \dots, R \quad (1)$$

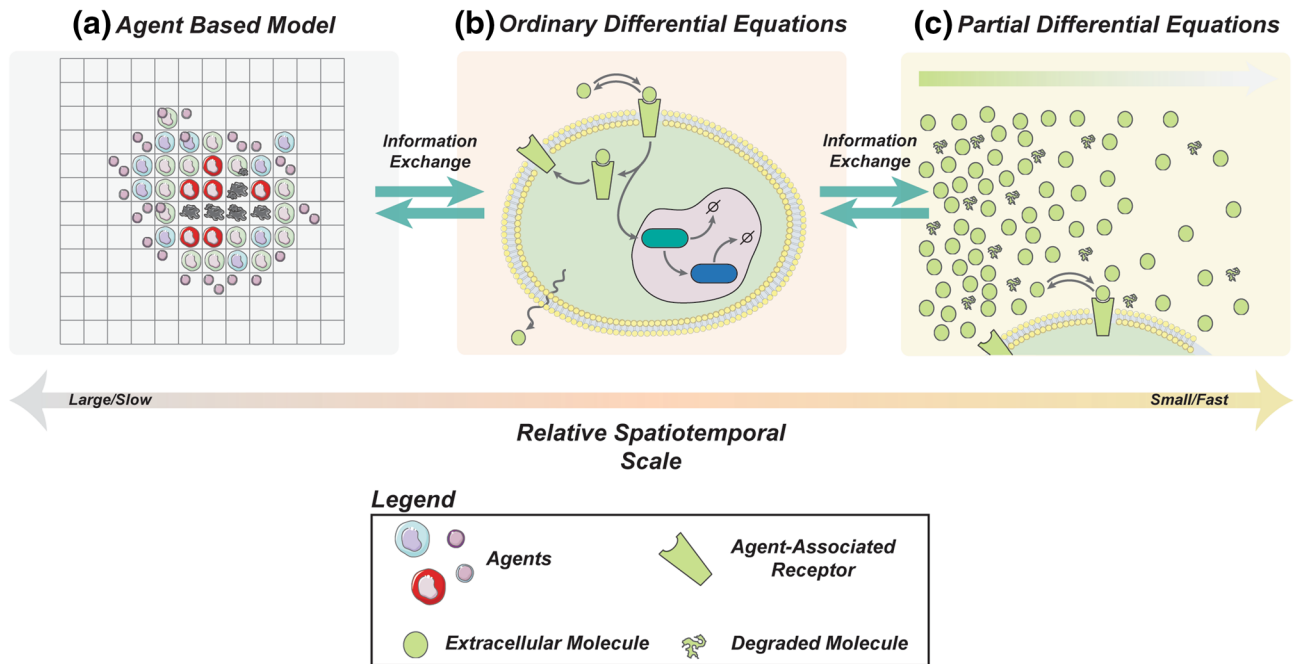


FIGURE 2. Mathematical representations of biological processes acting across different spatiotemporal scales. Individual scale models are combined with exchange of information across scales. (a) An ABM represents tissue and cellular scales (e.g., cell activation states). (b) Ordinary differential equation models represent molecular scale behaviors associated with cells (e.g., receptor-ligand trafficking and intracellular signaling). (c) Partial differential equation models represent molecular scale behaviors of the environment (e.g., extracellular molecule diffusion). Together these integrated individual scale models form the basis of a hybrid multi-scale ABM.

Equation (1) represents the agent-associated species (R total species), where Y_r is an agent-associated species, and t is time. L is an extracellular diffusing molecule (e.g., a ligand that binds to a surface receptor) that is modeled on a continuum scale, and β is a vector of rate parameters independent of t and Y_r . f_r is a function of agent-associated species, diffusing molecules, and rate parameters (e.g., as necessary for zeroth, first, or second order reaction kinetics). β is dependent upon the state of the agent (V), and thus rate parameters can change when an agent changes state. Multiple diffusing molecules can be included, although in our examples we will only include one for simplicity. The agent-associated reactions describe reactions occurring in agents, such as cell-cycle proteins controlling proliferation or actin remodeling controlling cellular movement.^{2,93} More common is a description of receptor-ligand binding and trafficking and ensuing intracellular signaling processes, as in the three examples given above.^{10,14,28,49,84} These reactions are typically based on mass-action kinetics.⁵¹ A simple example of receptor-ligand binding, trafficking, and intracellular signaling reactions for a single agent is given in Table 1.

Agent-associated reactions are dependent upon the local concentration of extracellular diffusing molecules (L) (Eq. (1)). These molecules diffuse and degrade in

the extracellular environment, and are typically described by continuum equations. The linked mathematical representation is a diffusion–reaction equation:

$$\frac{\partial L(x, y, t)}{\partial t} = D \nabla^2 L(x, y, t) - k_{\text{deg}} L(x, y, t) + \sum_{A(x, y, V)} (g(L, Y_1, Y_2, \dots, Y_R, \beta)) \quad (2)$$

where D is the isotropic diffusion coefficient, k_{deg} is the extracellular degradation rate constant, and $g(L, Y_1, Y_2, \dots, Y_R, \beta)$ is the effect agent-associated reactions (Eq. (1)) on the concentration of extracellular diffusing molecules.^{13,51} For instance, secretion of extracellular ligand or dissociation of ligand from cell surface receptors will increase the concentration of extracellular diffusing molecules, while binding will decrease it. Conversions to correct units are necessary as agent-associated quantities are usually given on a per cell basis (e.g., #/cell), while extracellular diffusing molecules are typically described by concentration in the extracellular space (e.g., nM) (see Table 1). This mathematical formulation allows each agent to interact with extracellular diffusing molecules in the environment through agent-associated molecules unique to each agent, $A(x, y, V)$. This gives the dynamic exchange of information between differential equation models

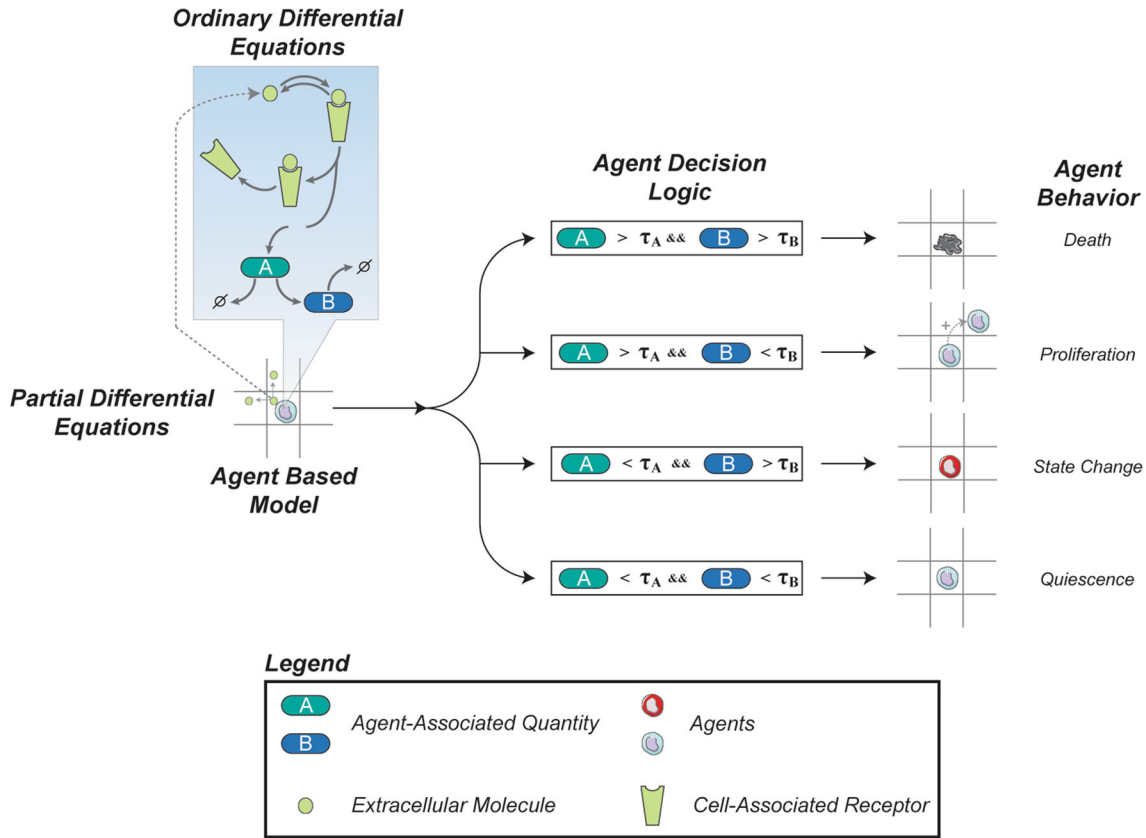


FIGURE 3. Example of how information is exchanged across scales in a hybrid multi-scale ABM. Extracellular molecules in the environment (with diffusion and degradation described using partial differential equations) interact with agents through agent-associated reactions (ordinary differential equations). Based on relative levels of agent-associated species (species A, green and species B, blue) agents make different decisions: (1) if both species A and B are above specified thresholds the agent will die, (2) if only species A (green) is above the specified threshold the agent will proliferate, (3) if only species B (blue) is above the specified threshold the agent will change state, (4) if both species A and B are below specified thresholds the agent will be quiescent. Agent decision logic using thresholds is only one example of how agent-associated reactions can be linked to various dynamics. Other examples include Poisson processes based on agent-associated quantities and rate of change of agent-associated species.^{26,28,89} Figure style partially adapted from Ref. 89.

and the ABM, as Eqs. (1) and (2) are dependent upon both agents and extracellular diffusing molecules. Agents are moving, interacting, and changing state in the ABM with a simultaneous and direct interface with extracellular diffusing molecules. Changes to concentrations of extracellular diffusing molecules in the environment factor into the agent decision-making processes, while changes in agent-associated reactions can influence agent states (Fig. 3).

Operator Splitting

We can use temporal operator splitting to decouple Eq. (2) into simpler and more tractable systems for numerical solution.^{16,38,54,59,80,82} Here, we split Eq. (2) into three equations: (1) extracellular molecule diffusion (operator Θ_1), (2) agent-associated reactions (operator Θ_2), and (3) extracellular molecule degradation (operator Θ_3). Therefore, Eq. (2) becomes:

$$\frac{\partial L(x, y, t)}{\partial t} = D \nabla^2 L(x, y, t) = \Theta_1 \quad (3)$$

$$\sum_{A(x,y,V)} \frac{dL(x,y,t)}{dt} = g(L, Y_1, Y_2, \dots, Y_R, \beta) \quad (4)$$

$$\frac{dY_r}{dt} = f_r(L, Y_1, Y_2, \dots, Y_R, \beta) \quad r = 1, 2, \dots, R$$

$$\frac{\partial L(x, y, t)}{\partial t} = -k_{\text{deg}} L(x, y, t) = \Theta_3 \quad (5)$$

The agent-associated reactions, f_r , (Eq. (1)) and the effect of agent-associated reactions, g , (Eq. (2)) on the extracellular diffusing molecule must be solved together as the equations depend on quantities from both equations (Eq. (4)). This reduces the problem to solving a partial differential equation (PDE) (Eq. (3)), a set of non-linear ordinary differential equations (ODEs) for each agent (Eq. (4)), and a simple linear

first order ODE (Eq. (5)). Equation (5) has an analytical solution:

$$L(x, y, t) = L(x, y, t_0)e^{-k_{\text{deg}}t} \quad (6)$$

The remaining equations, Eqs. (3) and (4) (such as those shown in Table 1), can now be solved using existing numerical methods and discrete time steps. The overall numerical approximation to Eq. (2) is then obtained by mathematically combining the solution to each individual equation (Eqs. (3), (4), and (5)). The splitting method determines the accuracy of the overall solution and also determines relative time steps used for the individual equations.

Lie splitting (also known as first-order splitting) is the most commonly used method in multi-scale ABMs. As shown in Fig. 4, the solution to each individual equation is estimated in sequence using the same time step (Δt), with the solution of each operator as the input to the next operator^{26,38,59}:

$$\Theta_1(\Delta t) \rightarrow \Theta_2(\Delta t) \rightarrow \Theta_3(\Delta t) \approx \Theta(\Delta t) \quad (7)$$

Lie splitting has first order accuracy with solution error due to splitting of Eq. (2) being proportional to the discrete time step $O(\Delta t)$.^{26,38,59}

A simple improvement over Lie splitting is Strang splitting (Eqs. (8), (9)), shown in Fig. 4, which is second order accurate $O(\Delta t^2)$ ⁸⁰:

$$\Theta_2\left(\frac{\Delta t}{2}\right) \rightarrow (\Theta_1(\Delta t) \rightarrow \Theta_3(\Delta t)) \rightarrow \Theta_2\left(\frac{\Delta t}{2}\right) \approx \Theta(\Delta t) \quad (8)$$

$$\Theta_2\left(\frac{\Delta t}{2}\right) \rightarrow \Theta_4(\Delta t) \rightarrow \Theta_2\left(\frac{\Delta t}{2}\right) \approx \Theta(\Delta t) \quad (9)$$

The most computationally intensive operator is solved using the full time step (Δt), while the less computationally intensive operator is solved using a half time step ($\Delta t/2$). With three operators, two are grouped

together (in this case Θ_1 and Θ_3) and the splitting method is used on the combined operator (Θ_1 and Θ_3). The splitting between the Θ_1 and Θ_3 operators remains Lie splitting. We group the molecular diffusion operator (Θ_1) and the molecular degradation operator (Θ_3) together in all further sections and refer to the combined operator as Θ_4 . We advocate the use of Strang splitting as the increased accuracy provides increased flexibility in choosing appropriate time steps. We base all further analysis on implementation of Strang splitting.

While operator splitting makes Eq. (2) easier to solve, if too large of a time step (Δt) is chosen, one is essentially considering the system to be mathematically decoupled. This can lead to non-phenomenological behavior of the system. Additional operator splitting techniques have been developed and include higher order methods such as Yoshida splitting (fourth and sixth order), Kahan splitting, and Zassenhaus products.^{21,34,45,94} Although the accuracy of the splitting method increases with these methods, additional function evaluations (some requiring steps backwards in time) make them more complicated approaches.

Model Layers and Discretization

Hybrid multi-scale ABMs are implemented using multiple super-imposed layers of information.³⁸ We follow this methodology and describe two layers: an *environment layer* and an *agent layer*. The environment layer holds information for each extracellular diffusing molecule (L) and is discretized into grid points of uniform spacing, Δx and Δy (Fig. 5). The discretized grid is described using lattice parameters; i increases in the x -dimension and j increases in the y -dimension. Thus the local concentration of an extracellular molecule is given by $L_{i,j}$. The agent layer, also a discretized grid, holds positional information of the agents, providing a framework for agent movement, behavior, and interaction. Agents in the agent layer interact with the environment layer at their corresponding positions. We

TABLE 1. Example of agent-associated reactions: receptor–ligand binding, trafficking, and intracellular signaling.

Description	Equation
Diffusing molecule— $[L]$ (M)	$\frac{d[L]}{dt} = k_{\text{synth}} - (\rho/N_{\text{AV}})(k_{\text{f}}[L][Y_1] + k_{\text{r}}[Y_2])$
Free receptor— $[Y_1]$ (#/cell)	$\frac{d[Y_1]}{dt} = -k_{\text{f}}[L][Y_1] + k_{\text{r}}[Y_2] + k_{\text{rec}}[Y_3]$
Bound receptor— $[Y_2]$ (#/cell)	$\frac{d[Y_2]}{dt} = k_{\text{f}}[L][Y_1] - k_{\text{r}}[Y_2] - k_{\text{int}}[Y_2]$
Internalized receptor— $[Y_3]$ (#/cell)	$\frac{d[Y_3]}{dt} = k_{\text{int}}[Y_2] - k_{\text{rec}}[Y_3]$
Signaling molecule— $[Y_4]$ (#/cell)	$\frac{d[Y_4]}{dt} = k_{\text{sig}}[Y_3] - k_{\text{dec}}[Y_4]$
Response factor— $[Y_5]$ (#/cell)	$\frac{d[Y_5]}{dt} = k_{\text{resp}}[Y_4] - k_{\text{d}}[Y_5]$

k_{f} , association rate constant (1/M s); k_{r} , dissociation rate constant (1/s); k_{int} , internalization rate constant (1/s); k_{rec} , recycling rate constant (1/s); k_{synth} , synthesis rate constant (#/cell s); k_{sig} , signaling rate constant (1/s); k_{dec} , signal decay rate constant (1/s); k_{resp} , signal response rate constant (1/s); k_{d} , response decay rate constant (1/s); ρ (cells/L), N_{AV} , Avogadro's constant (#/mol).

prefer to maintain the same discretization size for both agent and environment layer, due to the simplicity in mapping between the two layers. Different discretization sizes of the environment and agent layers (Δx , Δy) have been used in the context of a hybrid multi-scale ABM but require interpolation between agent and environment layers.³⁸

Tuneable Resolution

As more agent-associated reactions and species are included in Eq. (4) (see Table 1), the computational cost of solving the equations grows. Each additional reaction or species must be solved for every agent in the system; in published models the number of agents ranges from a few hundred to as many as 100,000. Tuneable resolution is an approach that advocates reducing the complexity of a system by ‘coarse-graining’ a detailed model (or aspects of that model) to save computational resources while preserving key mechanisms and behaviors.⁴⁹ For instance, an initial and fairly simple or ‘coarse-grained’ model is developed and the computational cost associated with solving the model is acceptable. Spurred by more biological data or additional questions, a more detailed or ‘fine-grained’ model containing many more agent-associated reactions is formulated, but it requires significant computational resources to solve. For subsequent biological questions, however, all of the detail of this ‘fine-grained’ model may not be needed. The goal is to use the ‘fine-grained’ model to build a better ‘coarse-grained’ model that estimates key mechanisms and behaviors from the ‘fine-grained’ model while simultaneously alleviating computational burdens (and facilitating model sharing and analysis). For example,

it may be reasonable to assume pseudo steady-state for some agent-associated reactions or to use an apparent or lumped rate constant to approximate a set of reactions; sensitivity analysis and consideration of time scales may aid in these decisions.^{35,49,55,64}

NUMERICAL METHODS FOR PDE SUB-MODELS

To solve the two-dimensional form of Eq. (3) in Cartesian coordinates (Eq. (10)) one can utilize either explicit (the solution at a later time point can directly be computed from the current state of the system) or implicit (the solution at a later time point is calculated from both the current state of the system and the solution at the later time point) methods.

$$\frac{\partial L(x, y, t)}{\partial t} = D \left(\frac{\partial^2 L(x, y, t)}{\partial x^2} + \frac{\partial^2 L(x, y, t)}{\partial y^2} \right) \quad (10)$$

As explicit methods are more straightforward and also do not require linear algebra solvers, these methods are relatively easy to incorporate into a hybrid multi-scale ABM. Thus, we describe the basis and central features of three explicit methods: Forward-Time Central-Space, Alternating-Direction Explicit, and Spectral.

Forward-Time Central-Space Method

The simplest and most frequently used numerical method for solving diffusion equations in the context of a hybrid multi-scale ABM is the forward-time central-space (FTCS) approximation.^{9,26,38} FTCS is an explicit method (the concentration at the next time step can be directly calculated from concentrations at the current

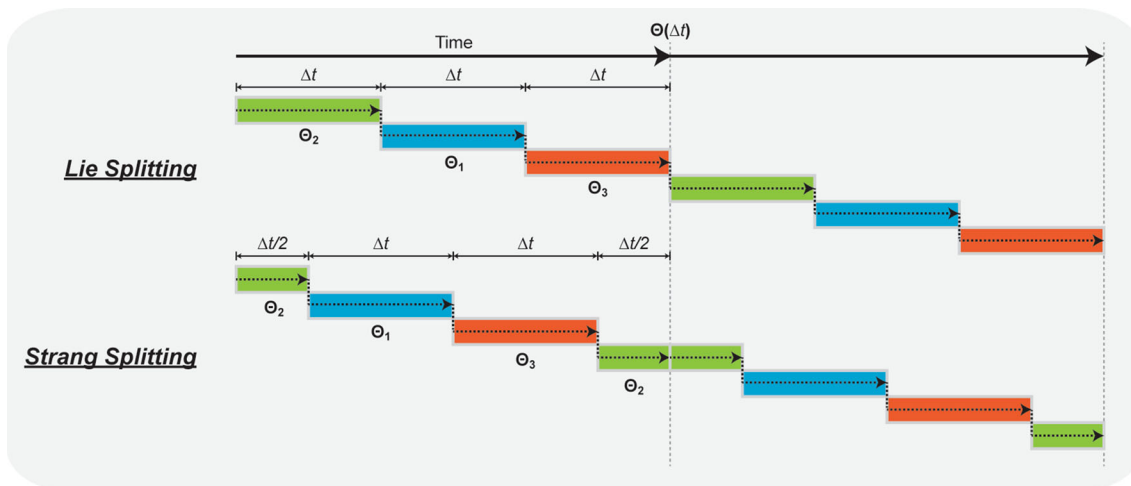


FIGURE 4. Operator splitting algorithms. The top panel represents Lie Splitting, where each operator (θ_1 , θ_2 , and θ_3) is advanced in time one after the other. The bottom panel represents Strang splitting, where one operator (θ_2) is advanced halfway in time, followed by the other operators being advanced all the way in time (θ_1 and θ_3), and then the first operator (θ_2) is advanced another half-step in time.

time step) that uses a first order forward approximation of the time derivative and a second order central difference approximation of the spatial derivatives.^{9,66} FTCS requires the discretized grid concentrations ($L_{i,j}$) in the environment layer to be stored for both the current time point (t) and the next time point ($t + \Delta t$). Insulating boundary conditions are applied by ensuring the flux across the boundary is zero, while Dirichlet boundary conditions are applied by setting the appropriate concentration at the boundary.

The FTCS method is $O(\Delta t)$ accurate in time and $O(\Delta x^2, \Delta y^2)$ in space, while the computational cost is $O(n^2)$ per time step. The FTCS method is numerically stable only if the following criterion is met:

$$D\Delta t \left(\frac{1}{\Delta x^2} + \frac{1}{\Delta y^2} \right) \leq \frac{1}{2} \quad (11)$$

Therefore, the time step is directly dependent upon the diffusivity of the extracellular molecule in the environment (e.g., larger diffusivities mean lower time steps).

Alternating-Direction Explicit Method

The alternating-direction explicit (ADE) numerical method is an extension of the FTCS method built upon the Peaceman–Rachford alternating direction concept.^{9,62} Let both $u_{i,j}$ and $v_{i,j}$ be finite difference approximations of the extracellular molecule concentration, $L(x,y,t)$.

$$\frac{u_{i,j}^{t+\Delta t} - u_{i,j}^t}{\Delta t} = D \left(\frac{u_{i+1,j}^t - u_{i,j}^t + u_{i-1,j}^{t+\Delta t} - u_{i,j}^{t+\Delta t}}{\Delta x^2} + \frac{u_{i,j+1}^t - u_{i,j}^t + u_{i,j-1}^{t+\Delta t} - u_{i,j}^{t+\Delta t}}{\Delta y^2} \right) \quad (12)$$

$$\frac{v_{i,j}^{t+\Delta t} - v_{i,j}^t}{\Delta t} = D \left(\frac{v_{i+1,j}^{t+\Delta t} - v_{i,j}^{t+\Delta t} + v_{i-1,j}^t - v_{i,j}^t}{\Delta x^2} + \frac{v_{i,j+1}^{t+\Delta t} - v_{i,j}^{t+\Delta t} + v_{i,j-1}^t - v_{i,j}^t}{\Delta y^2} \right) \quad (13)$$

In the case of u , iteration proceeds in both the forward i and j directions. Thus, the values in Eq. (12) $u_{i-1,j}^{t+\Delta t}$ and $u_{i,j-1}^{t+\Delta t}$ are known from previous calculations when iterating forward through the grid. In the case of v , iteration proceeds in the reverse i and j directions (i.e., iterating backwards through the grid). Thus, the values in Eq. (13) at $v_{i+1,j}^{t+\Delta t}$ and $v_{i,j+1}^{t+\Delta t}$ are known from previous calculations when iterating backwards through the grid. Boundary conditions are set in the same manner as the FTCS method. The extracellular molecule concentration at the next time point, $L_{i,j}^{t+\Delta t}$, is calculated by averaging $v_{i,j}^{t+\Delta t}$ and $u_{i,j}^{t+\Delta t}$. The ADE method requires values to be stored for $u_{i,j}$, $v_{i,j}$, and $L_{i,j}$ for both the current time point (t) and the next time point ($t + \Delta t$) in the environment layer.

The ADE method is $O(\Delta t^2)$ accurate in time and $O(\Delta x^2, \Delta y^2)$ in space, i.e., it is more accurate than the FTCS method, but the computational cost remains $O(n^2)$ per time step. Furthermore, the ADE method is an explicit method that is unconditionally numerically stable (typically seen with implicit methods), which does not place a restriction on Δt .⁹ Thus, Δt can be chosen based solely on the accuracy of the solution needed. A maximum Δt of approximately 4–6 times the Δt predicted by the conditional stability criterion of the FTCS method (Eq. (11)) can be used for the ADE method while maintaining acceptable accuracy.^{9,18}

Spectral Methods—Discrete Sine and Cosine Transforms

Spectral methods solve PDEs by assuming the solution is a sum of basis functions and choosing basis coefficients in order to best satisfy the solution.^{19,31,85} Spectral methods reduce PDEs to ODEs, greatly diminishing the difficulty of computation.⁶⁰ The

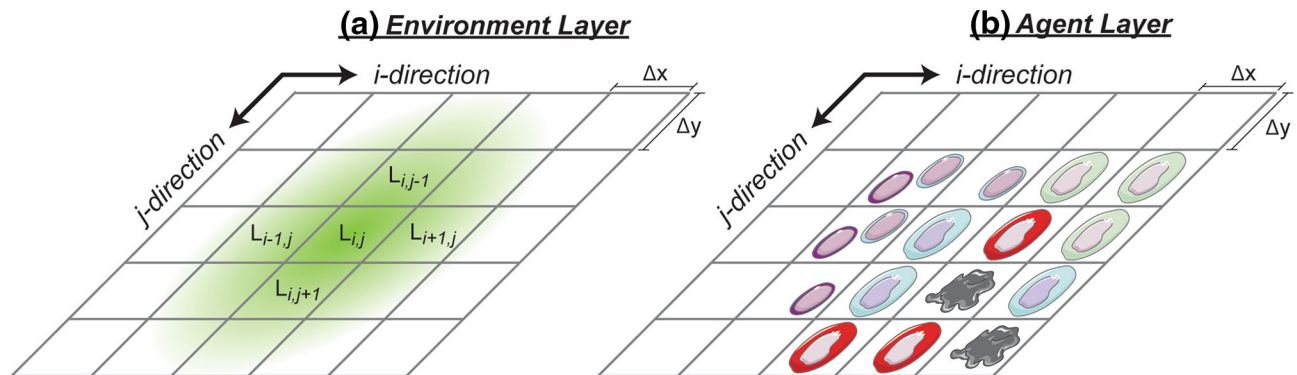


FIGURE 5. Model layers and discretization. Implementation of multiple layers holding different types of information (extracellular molecule concentration, L) discretized into grid of spacing Δx and Δy represented by i, j coordinates. (a) The environment layer represents the extracellular space of the hybrid ABM and holds extracellular molecule concentrations. (b) The agent layer holds positional information of agents. Agents in the agent layer interact with the environment layer at their corresponding positions.

two-dimensional discrete sine transform (DST) and discrete cosine transform (DCT) are defined as:

$$L_{i,j}^t = \sum_{k=0}^{M-1} \sum_{l=0}^{N-1} \bar{A}_{k,l} \sin\left(\frac{\pi}{M+1}(k+1)(i+1)\right) \sin\left(\frac{\pi}{N+1}(l+1)(j+1)\right) \quad (14)$$

$$L_{i,j}^t = \sum_{k=0}^{M-1} \sum_{l=0}^{N-1} \bar{A}_{k,l} \cos\left(\frac{\pi}{M-1}(k)(i)\right) \cos\left(\frac{\pi}{N-1}(l)(j)\right) \quad (15)$$

where k and l are the spectrally transformed i and j discretization, M and N are the lengths of k and l , and $\bar{A}_{k,l}$ are the spectral coefficients. The DST is an even-valued function at $k = -1$, $k = M$, $l = -1$, and $l = N$ which naturally applies a Dirichlet boundary condition (constant zero concentration). The DCT is an odd-valued function at $k = -1$, $k = M$, $l = -1$, and $l = N$ which naturally applies a Neumann boundary condition (insulating).

The appropriate transform (depending on the boundary condition for the modeled situation) is applied to Eq. (10) and the resulting ODE is solved analytically, given below.¹⁹

$$\bar{A}_{k,l}^{t+\Delta t} = \bar{A}_{k,l}^t e^{-P_{i,j}\Delta t} \quad (16)$$

In the case of the DST (Eq. (17)) and DCT (Eq. (18)):

$$P_{i,j} = \frac{2D}{\Delta x \Delta y} \left\{ 2 - \left(\cos\left(\frac{\pi(i+1)}{M+1}\right) + \cos\left(\frac{\pi(j+1)}{N+1}\right) \right) \right\} \quad (17)$$

$$P_{i,j} = \frac{2D}{\Delta x \Delta y} \left\{ 2 - \left(\cos\left(\frac{\pi(i)}{M-1}\right) + \cos\left(\frac{\pi(j)}{N-1}\right) \right) \right\} \quad (18)$$

$P_{i,j}$ is invariant and can be calculated from the discretization of the simulation space and the diffusion coefficient of the extracellular molecule. The spectral coefficients $\bar{A}_{k,l}^t$ can be determined using a Fast Fourier Transform (FFT) and advanced forward in time using Eq. (16). The spectral coefficients $\bar{A}_{k,l}^{t+\Delta t}$ can be converted back into extracellular molecule concentrations ($L_{i,j}$) using an inverse Fast Fourier Transform (FFT).²⁵ The FFTw library provides a simple C++ interface for computing spectral coefficients and their inverses.^{19,33} Using FFTw algorithms the computational cost for the forward and inverse FFTs are $O(n \log n)$, however multiplication of $\bar{A}_{k,l}^t$ with $P_{i,j}$ is $O(n^3)$ per time step.³³ Therefore, the overall cost of the spectral method is dominated by the multiplication cost of $O(n^3)$ per time step.

Spectral methods require the extracellular molecule concentrations to be stored at (t) and $(t + \Delta t)$ in the environment layer. Stability requirements are typically determined by examining the solution with different combinations of time step and discretization size.^{19,31} The accuracy of spectral methods is difficult to relate to O notation, but numerical errors tend to decay exponentially leading to much greater accuracy than purely finite difference methods.^{19,31,85} However, spectral methods have difficulty handling discontinuities or shock-like behaviors in input matrices and produce artifacts (or aliasing) at jump discontinuities, known as the ‘Gibb’s Phenomenon’.^{19,37,85} As the input concentration field into spectral methods can be fairly discontinuous a technique known as smoothing (or anti-aliasing) is applied to alleviate these issues.⁴³ The most common smoothing method is the ‘2/3’ rule, yet its computational cost can be large.⁴³ We have successfully implemented a simple smoothing method in hybrid multi-scale ABMs by using the FTCS method presented above.⁶⁴ We take between 2 and 5 FTCS algorithm steps before solving Eq. (10) using spectral methods. The number of FTCS steps is estimated by comparing the differences in the concentration field solution from a different method (e.g., FTCS or ADE) to the smoothed spectral method concentration field solution.

Other Available Numerical Methods

Implicit and semi-implicit algorithms (e.g., Crank–Nicholson) have also been used in hybrid multi-scale ABMs due to their stability characteristics.^{32,92,95} While increased stability allows for larger time steps, the need to assemble and determine a Jacobian matrix along with incorporating linear algebra solvers for systems of equations can be a complex task. Many libraries are available (e.g., LAPACK, LINPACK, PETSc, and GSL), but adapting existing code to libraries can be difficult. In the context of building a new hybrid multi-scale ABM or extending an existing ABM, in our experience it is much easier to use explicit schemas. Other advancements in solving PDEs are the multigrid and discrete wavelet transform (DWT) methods. The multigrid method has been demonstrated in the context of hybrid multi-scale ABMs.^{46,91,92} Implementation of the algorithm without libraries could be challenging, and available libraries (PETSc, Dune, Trilinos, FETK) may be difficult to interface with existing code. The DWT captures information in both the frequency and time domain, unlike the DCT and DST which capture only frequency information.²³ Thus, the DWT can handle local discontinuities better than spectral methods

while still using similar methods to compute wavelet coefficients at an $O(n \log n)$ or even $O(n)$ computational cost. DWTs are still relatively new and have yet to be applied in the context of a hybrid multi-scale ABM. Additionally, only limited libraries exist presenting a barrier to efficient usage. We are currently evaluating the possible benefits of both the multigrid and DWT algorithms in the context of solving extracellular molecule diffusion in hybrid multi-scale ABMs.

NUMERICAL METHODS FOR ODE SUB-MODELS

Equation (4) is a description of any agent-associated reactions and must be solved for each agent in the simulation. For ease of explanation we present the numerical methods in the context of a single agent in vector notation (Eq. (19)):

$$\frac{d\vec{Y}}{dt} = f(L, \vec{Y}, \vec{\beta}) \quad (19)$$

Forward Euler

The simplest and easiest algorithm to implement is the forward Euler (FE) method, which uses a forward finite difference estimation of the first order derivative in Eq. (19).⁶⁶ FE is an explicit method and only requires the concentrations of each species at the current time point (t) and an estimate of the derivative at the current time point. FE is $O(\Delta t)$ accurate in time and its computational cost is $O(n)$ per time step. The FE method is conditionally stable and is numerically unstable for stiff equations and large time steps. The criteria for numerical stability of the solution of a set of linear ODEs is given by:

$$|1 + \lambda\Delta t| < 1 \quad (20)$$

where λ is the set of eigenvalues for the system.⁷² For non-linear systems of ODEs (as in Table 1) the equations can be linearized and the behavior of the linearized system analyzed for stability, giving an approximate local stability criteria for the non-linear system.⁵² In practice this can be difficult for large systems of ODEs, and hence the stability limit for a particular set of ODEs is typically determined by trial-and-error.⁶⁹ Numerical stability requirements of the FE method in no way guarantee accuracy of the solution.

FOURTH ORDER RUNGE-KUTTA

Runge-Kutta methods use higher-order terms from the Taylor-series expansion of the first derivative. The

higher order terms are evaluated at distinct points and subsequently combined to give a better approximation to the first derivative.^{66,72} Most commonly used is the fourth order Runge-Kutta (RK4) method that requires concentrations of each species at the current time point (t) along with four estimates of the derivative. The RK4 method is $O(\Delta t^4)$ accurate in time, a significant improvement on the FE method. The computational cost of RK4 remains $O(n)$ per time step and is a conditionally stable method. The criteria for numerical stability of linear ODEs is shown below, where λ is the set of eigenvalues for the system⁵²:

$$(1 + \lambda\Delta t) + \frac{1}{2}(\lambda\Delta t)^2 + \frac{1}{6}(\lambda\Delta t)^3 + \frac{1}{24}(\lambda\Delta t)^4 < 1 \quad (21)$$

As mentioned above, biological systems are in general non-linear; therefore in practice the stability limit is again determined by trial-and-error.⁶⁹

Other Available Numerical Methods

A simple extension of the RK4 method is an adaptive step size Runge-Kutta method, known as RK4-5.^{66,77,78,96} This method determines the necessary time step for a given accuracy on-the-fly based on estimates of local error by calculating both the fourth order and fifth order Runge-Kutta solutions. The additional computational cost in calculating both fourth and fifth order solutions, estimating error, and determining the correct time step could be outweighed by significantly larger time steps. Implicit algorithms for solving ODEs can also be used.^{16,32,41,58,59,61,92} Similar to PDE algorithms, implicit algorithms require determining a Jacobian matrix and implementation of linear algebra solvers. Considering the large number of agents per simulation (anywhere from 100 to 100,000 s), assembly and solution of the Jacobian matrix can be an overwhelming task. Recently, some have suggested the use of *in situ* adaptive tabulation (ISAT) to minimize the number of numerical method calls.^{15,22,39,40,65,75} ISAT functions by tabulating existing solutions and determining appropriate regions of solution space where use of existing solutions or simple interpolation can accurately represent the solution without ever calling the numerical method.^{65,75} ISAT has not been demonstrated in the context of hybrid multi-scale ABMs but the theoretical reduction in computational cost is enticing. Lastly, many external programs and frameworks for solving systems of ODEs, such as MATLAB, COPASI, and CVODE,^{1,22,42,81,87} exist and could be linked to a hybrid multi-scale ABM. In our experience linking external programs to existing code can be difficult and may confer a large computational cost associated with module communication.

SYNCING NUMERICAL METHODS IN HYBRID MULTI-SCALE ABMS

It is critical to maintain *sync points* where differing time steps used to solve the PDEs, ODEs, and ABM are reconciled, thus linking the mathematics, exchanging information across scales, and allowing the model to correctly proceed forward in time. A challenge of hybrid multi-scale ABMs is to determine the largest time step for each numerical method that maintains easily identifiable sync points. For instance, a numerical method that solves extracellular molecule diffusion with a large time step requires fewer sync points with the agent-associated reactions (Fig. 6a) than a numerical method that solves extracellular molecule diffusion with a smaller time steps (Fig. 6b). A simple procedure for determining time steps that maintain sync points is given below. We assume Strang splitting and a previously determined time step for the ABM, Δt_{agent} :

1. Estimate the maximum time step to solve the extracellular molecule diffusion and degradation (Θ_4) for the chosen numerical method. A good starting point for all numerical methods is Eq. (11). Reduce the estimated time step to a number divisible by Δt_{agent} for syncing and set this value as Δt_{pde} .
2. Estimate the maximum time step, Δt_{ode} , to solve the ODE model of agent-associated reactions (Θ_2) for the chosen numerical method. This can be accomplished by linearizing the equations and using Eq. (20) or Eq. (21) or by using trial-and-error in a ‘test-bed’ environment such as a standalone implementation of the numerical method in C++ or MATLAB (The Mathworks Inc.—Natick, MA). Frequently, the maximal time step for numerical accuracy and stability will be significantly smaller than $\Delta t_{\text{pde}}/2$. Choose Δt_{ode} such that stability and accuracy requirements are satisfied. Additionally reduce Δt_{ode} to a number that is evenly divisible by $\Delta t_{\text{pde}}/2$ for syncing.
3. Using the estimated time steps (Δt_{agent} , Δt_{pde} , and Δt_{ode}) solve the hybrid ABM.
4. Reduce all time steps by a factor of 2 and re-solve the system.
5. Compare the model solutions. If the solutions are inconsistent the time steps are too large. Reduce all time steps (Δt_{pde} and Δt_{ode}) and re-verify that each is able to ‘sync’. Repeat steps 3–5 until the model solutions are within the desired tolerance.

A full hybrid multi-scale ABM algorithm is shown in Fig. 7 and includes: the agent time step, Δt_{agent} (agents move, change state, etc.), the ODE time step, Δt_{ode} (agent-associated reactions), and the PDE time step, Δt_{pde} (diffusion and degradation). Although not

the focus of this review, we note that successfully linking and solving a hybrid multi-scale ABM does not of course guarantee fidelity to data or its usefulness. Extensive model validation and testing are necessary using methods such as uncertainty and sensitivity analysis or non-linear least squares⁵⁶; individual scale models may function differently in the context of the integrated model. Examples of model validation can be found in particular applications^{8,18,44} and a broader discussion of some points can be found in Refs. ^{44,49}.

CASE STUDY: AN EXAMPLE HYBRID MULTI-SCALE ABM

Choosing numerical methods that maintain computational tractability of a hybrid multi-scale ABM is essential. Considerations affecting the choice of numerical methods include: number of agents, number of agent-associated reactions, and model dimensionality (i.e., 2D or 3D). In addition, uncertainty and sensitivity analysis is commonly used to understand how variations in parameter values affect model results and necessitates large numbers of model simulations ($\sim 10^3$).⁵⁶ In practice, hybrid multi-scale ABMs that require over a day to run severely limit model usefulness.

As a case study of the application of numerical methods described above, we ran comparison simulations with a hybrid multi-scale ABM of *M. tuberculosis* infection discussed earlier^{18,26,28,64} (Tables 2 and 3). Depending on the computational environment (i.e., computing cluster vs. laptop) and the processes modeled (e.g., number of extracellular diffusing molecules modeled on a continuum scale) the computational cost will vary greatly. However, this case study functions to illustrate the principles presented above and demonstrate the trade-offs between complexity of numerical algorithms (and implementation) and computational cost. The hybrid multi-scale ABM is constructed using the C++ programming language, Boost libraries (distributed under the Boost Software License—www.boost.org), FFTw libraries (distributed under GPL—www.fftw.org), and the Qt framework for visualization (distributed under GPL—www.qt.digia.com). The ABM is cross-platform (Macintosh, Windows, Unix) and can be run with or without our visualization software. Simulations were performed on the Flux high performance computing cluster, provided by Advanced Research Computing at the University of Michigan (<http://goo.gl/WQIyCX>). Computational accuracy was assessed by comparing output generated with different numerical methods, different platforms, and over different model resolutions. We also test individual sub-models for numerical

convergence outside of the multi-scale model (e.g., solving the ODEs or PDEs in MATLAB). However, methods to validate numerical convergence inside hybrid multi-scale ABMs need to be developed.

In Case Study 1 (see Table 2), we simulate 100 days of the immune response following an initial infection with *M. tuberculosis*. Diffusion and degradation of three extracellular molecules (two cytokines and one chemokine) are tracked, and thirteen agent-associated differential equations describe receptor-ligand binding, trafficking and signaling of TNF and IL-10.¹⁸ Extracellular molecule diffusivities are $\sim 10^{-8}$ cm²/sec for cytokines and chemokines. In Case Study 2 (see Table 3), we simulate 50 days of the immune response following an initial infection with *M. tuberculosis* plus an additional 50 days of antibiotic treatment.⁶⁴ Diffusion and degradation of five extracellular molecules (two cytokines, one chemokine, and two antibiotics) are tracked, and thirteen agent-associated differential equations describe receptor-ligand binding, trafficking and signaling of TNF and IL-10. In addition, the model in Case Study 2 tracks the effects of antibiotics against bacteria. Extracellular molecule diffusivities for these antibiotics are $\sim 10^{-7}$ – 10^{-6} cm²/s. As antibiotics diffuse much faster through tissue than cytokines and

chemokines (they are much smaller molecules), smaller time steps must be used in the numerical methods.

We show relative computational speeds for both a 100×100 (4 mm²) and 200×200 (16 mm²) simulation grid. Model discretization length (Δx , Δy) of the environment and agent layers is 20 μ m. For the larger grid, the number of calculations is increased due to ~ 2 -fold more agents (the number of agents present is not an input to the simulations but rather is generated from the stochastic nature of the simulations) and 4-fold more simulation space. Additionally, we employed a tuneable resolution approach (assuming a pseudo steady state for multiple reactions and using apparent rate constants) to reduce the thirteen agent-associated differential equations to two agent-associated differential equations.⁶⁴ For both Case Studies 1 and 2, we show the mean computational time from 3 simulations for each of the 38 different combinations of numerical methods (including tuneable resolution). Tables 2 and 3 depict fold-changes in computational speed normalized to the slowest value for the specific grid size (i.e., higher values indicate shorter computation times). The standard deviations for simulations range from ± 1 to 30% of the mean computational time.

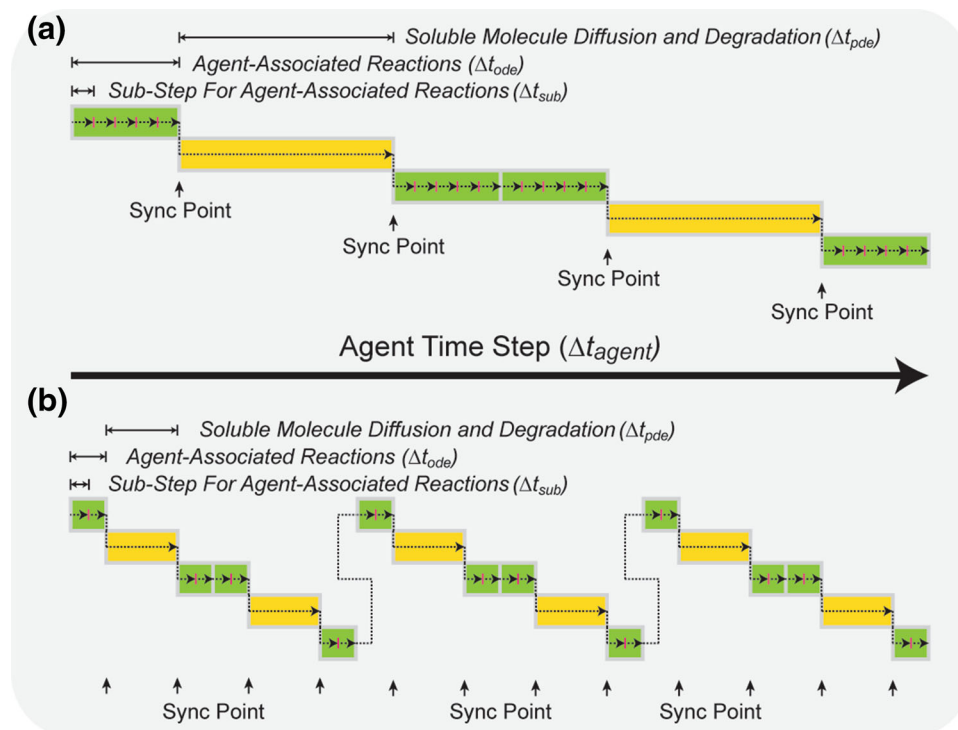


FIGURE 6. Syncing time steps across hybrid multi-scale ABMs. Example of two different combinations of time steps for extracellular molecule diffusion and agent-associated reactions. (a) A large time step for extracellular molecule diffusion requires few sync points with the agent-associated reactions. (b) A small time step for extracellular molecule diffusion requires many sync points with the agent-associated reactions.

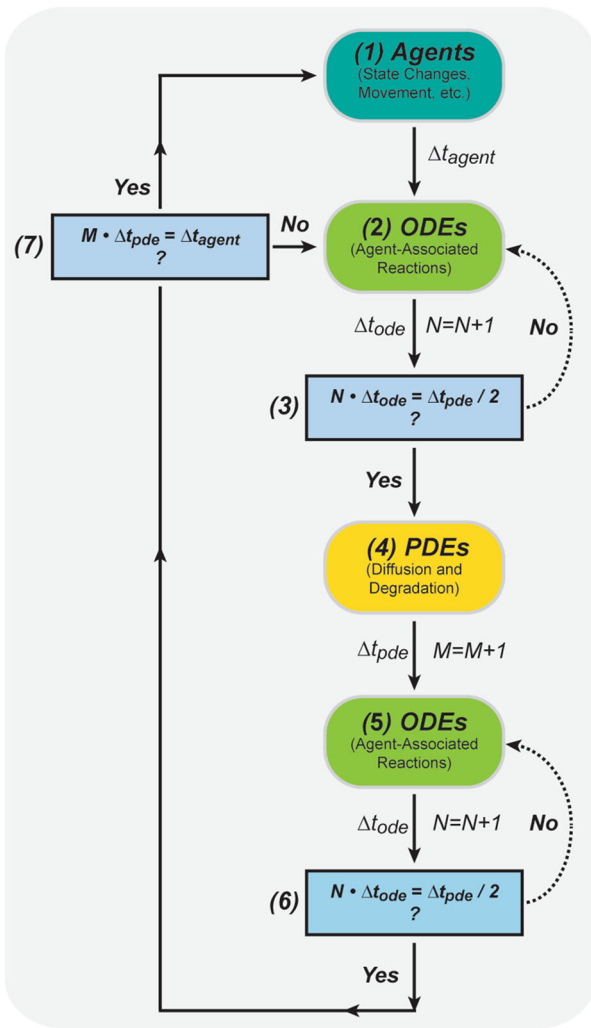


FIGURE 7. Diagram of a solution algorithm for a hybrid multi-scale agent-based. (1) Update agents (movement, states, proliferation, etc.). (2) Solve a single time step (Δt_{ode}) for agent-associated reactions (θ_2). Increment a counter N . (3) If the total time step ($N \times \Delta t_{ode}$) is equal to ($\Delta t_{pde}/2$) then move on to extracellular molecule diffusion and degradation. If not, take another single time step for agent-associated reactions (θ_2) and check again. (4) Solve a single time step (Δt_{pde}) for extracellular molecule diffusion and degradation. Increment a counter M . (5) Solve a single time step (Δt_{ode}) for agent-associated reactions (θ_2). Increment a counter N . (6) If the total time step ($N \times \Delta t_{ode}$) is equal to ($\Delta t_{pde}/2$) move on to the final check. If not, take another single time step for agent-associated reactions (θ_2) and check again. (7) If the total time step ($M \times \Delta t_{pde}$) is equal to (Δt_{agent}) then a full time step has been completed. Continue by updating agents as indicated in (1). If not, continue solving with step (2).

Our results in Tables 2 and 3 demonstrate that implementation of appropriate numerical methods and time steps can dramatically improve overall computational speed in hybrid multi-scale ABMs. Moving to more sophisticated numerical methods for solution both ODEs and PDEs increases computational speed by up to 5-fold in Case Study 1 or 25-fold in Case Study 2 (Tables 2 and 3). The benefits of a tuneable

resolution approach are easily observed, with an additional 2-fold to 5-fold increase in the computational speed beyond increases due to choice of numerical method (Tables 2 and 3). Although Case Study 1 does benefit from spectral methods, the diffusion time step cannot be increased (beyond ~ 120 s) as the mathematics begin to decouple at larger time steps (see “Operator Splitting” section). The diffusion time steps used in Case Study 2 are restricted to smaller values as antibiotics diffuse much faster than cytokines and chemokines in the environment. With these restrictions on diffusion time steps, decoupling is less of a concern in Case Study 2 and spectral methods are more advantageous than in Case Study 1. In both Case Studies a combination of tuneable resolution and spectral methods increases computational speeds more than 20-fold.

There are caveats to implementation of faster and more efficient numerical algorithms in the context of hybrid multi-scale ABMs. Increasing the efficiency of solving one operator (Eqs. (3)–(5)) is eventually limited by the efficiency of solving a different operator. For instance, implementing a spectral-based algorithm for solving the diffusion operator is of limited benefit if the agent-associated reactions (ODEs) are solved using a Forward Euler-based methodology (Table 2). Thus, improvements in one operator must also be thought of in the context of another operator, leading to a constant cycle of re-evaluation and implementation of numerical solvers.

Another critical aspect of solving hybrid multi-scale ABMs is the importance of correctly choosing algorithms with compatible time steps. The benefit of implementing a different numerical algorithm can be reduced if the algorithm cannot take sufficiently large time steps due to limitations of another numerical algorithm. For instance, in Case Study 2 using the RK4 algorithm to solve the agent-associated reactions could theoretically allow time steps upwards of 5-10 s. However, due to faster tissue diffusivity values of antibiotics (~ 10 -fold higher than cytokines and chemokines) if we use the FTCS algorithm to solve extracellular molecule diffusion, it limits use of larger time steps in the RK4 algorithm (Table 3).

Lastly, it is important to understand the computational costs associated with expanding the size of a model. In our Case Study, transitioning from a 100×100 to a 200×200 simulation grid reduces the computational speed ~ 7 -fold. We have also expanded the example hybrid multi-scale ABM to 3-dimensions (100×100 grid to $100 \times 100 \times 100$ grid), which reduced the computational speed ~ 42 -fold. Without *a priori* knowledge of the factors that contribute to computational costs, hybrid multi-scale ABMs may become too bulky or inefficient to provide novel

TABLE 2. Relative computational speeds for Case Study 1.

PDE numerical method	100 × 100 simulation grid–5000 agents			200 × 200 simulation grid–10,000 agents		
	ODE numerical method			ODE numerical method		
	FE ($\Delta t = 0.6$ s)	RK4 ($\Delta t = 6$ s)	TR ($\Delta t = 6$ s)	FE ($\Delta t = 0.6$ s)	RK4 ($\Delta t = 6$ s)	TR ($\Delta t = 6$ s)
FTCS ($\Delta t = 6$ s)	1.0	2.3	4.6*	1.0	2.6*	5.4*
ADE ($\Delta t = 30$ s)	1.8	4.3*	12.8*	1.2	3.9*	7.7*
SM ($\Delta t = 120$ s)	1.8	5.5*	22.7*	1.2	5.2*	23.6*

FTCS, forward time central space; ADE, alternating direction explicit; SM, spectral method; FE, forward Euler; RK4, Runge–Kutta fourth Order; TR, tuneable resolution.

$N = 3$ for all simulations. * indicates $p < 0.05$ based on students t test. SD is ± 1 –35% of mean computational time.

100 × 100—Relative Speed of 1.0 corresponds to 7589 s of simulation time.

200 × 200—Relative Speed of 1.0 corresponds to 46,907 s of simulation time.

TABLE 3. Relative computational speeds for Case Study 2.

PDE numerical method	100 × 100 simulation grid–5000 agents			200 × 200 simulation grid–10,000 agents		
	ODE numerical method			ODE numerical method		
	FE	RK4	TR	FE	RK4	TR
FTCS	(0.6/0.6) 1.4	(0.6/0.6) 1.0	(0.6/0.6) 1.5*	(0.6/0.6) 1.4	(0.6/0.6) 1.0	(0.6/0.6) 1.2
ADE	(3.0/0.6) 2.8*	(3.0/3.0) 3.2*	(3.0/3.0) 3.6*	(3.0/0.6) 3.1*	(3.0/3.0) 4.0*	(3.0/3.0) 4.9*
SM	(60/0.6) 6.8*	(60/6.0) 15.8*	(60/6.0) 43.8*	(60/0.6) 8.3*	(60/6.0) 26.3*	(60/6.0) 63.5*

(xx/xx) → (Soluble molecule diffusion time step/agent-associated reactions time step).

FTCS, forward time central space; ADE, alternating direction explicit; SM, spectral method; FE, forward Euler; RK4, Runge–Kutta fourth Order; TR, tuneable resolution.

$N = 3$ for all simulations. * indicates $p < 0.05$ based on students t test. SD is ± 1 –35% of mean computational time.

100 × 100—Relative Speed of 1.0 corresponds to 26,968 s of simulation time.

200 × 200—Relative Speed of 1.0 corresponds to 259,150 s of simulation time.

insights into the complex biological systems they represent.

DISCUSSION

Multi-scale models aim to replicate fundamental behaviors of biological systems, with constant exchange of information across scales, in order to better understand and predict system behavior as a whole. Coupling individual scale models, such as an ABM and differential equation models, to allow for the exchange of information, is typically accomplished by linking mathematical formulations across each scale. Thus, tools to link individual scale models and efficient methods of solving the subsequent linked models are important to advance the use of hybrid multi-scale ABMs in generating new biological knowledge from the wealth of available data.

Here, we describe the general framework for linking ABMs and differential equation models and solving the resulting hybrid multi-scale model, including layers, discretization, and operator splitting. The framework is extendable to different levels of model detail and adaptable to the focus and needs of the problem

(e.g., inclusion of antibiotic treatment in an infection model, or moving from two to three dimensions). We review three numerical algorithms for solving extracellular molecule diffusion and two numerical algorithms for solving individual agent-associated reactions. Additionally, we demonstrate the merits of a tuneable resolution approach to reduce the complexity of a system and limit computational cost.⁴⁹ We show how an appropriate choice of numerical algorithms and time steps can improve the computational tractability and efficiency of a hybrid multi-scale ABM. The most important factors in choosing these algorithms are: (1) familiarity with the underlying mathematics, (2) an understanding of relative process rates, and (3) computational resources such as time and power that are available. If unfamiliar with numerical methods, it is easier to implement an algorithm built around simple mathematical concepts, such as FTCS for solving extracellular molecule diffusion, than to start with a more mathematically sophisticated algorithm. As the user becomes comfortable with simpler implementations, more complex algorithms tend to build on simpler concepts in an incremental fashion. Second, it is necessary to have a basic understanding of relative rates (e.g., rates of diffusion compared to rates of

agent-associated reactions) in order to determine whether solution of a hybrid multi-scale ABM will benefit from a particular numerical algorithm. For instance, a small molecule drug diffuses through tissue much faster than a extracellular protein molecule (such as a cytokine) so implementing a method that solves the agent-associated reactions with a time step larger than the time step required for solving diffusion of the drug through tissue has limited benefits as the diffusive rate restricts the overall time step (Table 3). Lastly, it is important to note that the extent of computational resources available such as power and computational time needed for each model, as new numerical methods can have diminishing returns. For instance, running a sensitivity analysis requires a large number of model simulations (e.g., thousands of simulations). Therefore, implementing a new numerical method for aspects of a model will have more benefits in this case as compared to single simulations.

At present, ABM platforms and languages such as NetLogo or SPARK do not accommodate the framework described in this manuscript to develop a hybrid multi-scale ABM. While in principle one can link those platforms with other platforms, e.g., MATLAB for solving ODEs, in practice we have found this difficult, if not impossible, for our models. This is largely due to communication between software packages slowing down the models to the point of uselessness. Platforms such as CHASTE are making advances towards re-usable and non-specific hybrid multi-scale ABMs (e.g., the code is able to model both cardiac tissue and crypt formation); however, there is no ‘one-size fits all’ platform that is flexible enough for a user to easily develop a hybrid multi-scale ABM.^{29,83} Therefore, a short-term solution may be stripping away the biological system/disease state-specific portions of models and publishing a baseline mathematical framework for a hybrid multi-scale ABM that can be modified by the user to suit a particular application. Although not ideal this would speed up development of hybrid multi-scale ABMs and also lower the barrier to creation of new models by inexperienced users. Issues of model modularity and reproducibility are of great interest to the multi-scale biological modeling community (see the Interagency Modeling and Analysis Group website at <http://www.imagwiki.nibib.nih.gov>) and may spur the development of more user-friendly packages.⁶³

Multi-scale models are becoming a more prevalent tool to understand systems-level biological phenomena. Modeling efforts are driving biological research from a descriptive field to a predictive field, especially in the context of pharmaceutical research. The ability to unify genomic, proteomic, metabolomics data using modeling constructs is an emerging technique to facilitate new drug-development and discovery along

with new ways to re-purpose old drugs.^{12,47,53,58} Modeling approaches can predict new therapeutic targets by identifying key mechanisms of disease pathology, rapidly assess efficacy and toxicity of new drugs, or rapidly optimize drug concentrations and dosing schedules. We are only beginning to develop computational models capable of performing these studies. As more biological data are integrated into models and their complexity grows, efficient implementation of hybrid multi-scale ABMs becoming increasingly important. In this work, we demonstrate a framework and suggest tools that allow for efficient implementation of hybrid multi-scale ABMs to help guide the choice and development of both new model creation and existing platforms.

ACKNOWLEDGMENTS

We thank Paul Wolberg and Joe Waliga for computational assistance. This research was supported in part through computational resources and services provided by Advanced Research Computing at the University of Michigan, Ann Arbor. This research was funded by the following NIH Grants: R01 EB012579 (DEK and JLL) and R01 HL 110811 (DEK and JLL).

CONFLICT OF INTEREST

Nicholas Cilfone, Denise Kirschner, and Jennifer Linderman declare no conflicts of interests.

ETHICAL STANDARDS

No human or animal studies were carried out by the authors for this article.

REFERENCES

- ¹Adra, S., T. Sun, S. MacNeil, M. Holcombe, and R. Smallwood. Development of a three dimensional multi-scale computational model of the human epidermis. *PLoS ONE* 5:e8511, 2010.
- ²Alarcón, T., H. M. Byrne, and P. K. Maini. Towards whole-organ modelling of tumour growth. *Prog. Biophys. Mol. Biol.* 85:451–472, 2004.
- ³An, G., Q. Mi, J. Dutta-Moscato, and Y. Vodovotz. Agent-based models in translational systems biology. *Wiley Interdiscip. Rev. Syst. Biol. Med.* 1:159–171, 2009.
- ⁴Anderson, A. R. A., M. A. J. Chaplain, and K. A. Rejniak (eds.). *Single-Cell-Based Models in Biology and Medicine*. Birkhäuser Basel: Basel, 2007.
- ⁵Angermann, B. R., *et al.* Computational modeling of cellular signaling processes embedded into dynamic spatial contexts. *Nat. Methods* 9:283–289, 2012.

- ⁶Athale, C. A., and T. S. Deisboeck. The effects of EGF-receptor density on multiscale tumor growth patterns. *J. Theor. Biol.* 238:771–779, 2006.
- ⁷Athale, C., Y. Mansury, and T. S. Deisboeck. Simulating the impact of a molecular “decision-process” on cellular phenotype and multicellular patterns in brain tumors. *J. Theor. Biol.* 233:469–481, 2005.
- ⁸Bailey, A. M., M. B. Lawrence, H. Shang, A. J. Katz, and S. M. Peirce. Agent-based model of therapeutic adipose-derived stromal cell trafficking during ischemia predicts ability to roll on P-selectin. *PLoS Comput. Biol.* 5:e1000294, 2009.
- ⁹Barakat, H. Z., and J. A. Clark. On the solution of the diffusion equations by numerical methods. *J. Heat Transfer* 88:421, 1966.
- ¹⁰Basak, S., M. Behar, and A. Hoffmann. Lessons from mathematically modeling the NF- κ B pathway. *Immunol. Rev.* 246:221–238, 2012.
- ¹¹Bauer, A. L., C. A. Beauchemin, and A. S. Perelson. Agent-based modeling of host-pathogen systems: the successes and challenges. *Inf. Sci. (NY)* 179:1379–1389, 2009.
- ¹²Berg, E. L. Systems biology in drug discovery and development. *Drug Discov. Today* 19:113–125, 2013.
- ¹³Bird, R. B., W. E. Stewart, and E. N. Lightfoot. *Transport Phenomena*. New York: Wiley, 1994.
- ¹⁴Braun, D. A., M. Fribourg, and S. C. Sealfon. Cytokine response is determined by duration of receptor and signal transducers and activators of transcription 3 (STAT3) activation. *J. Biol. Chem.* 288:2986–2993, 2013.
- ¹⁵Chakrabarti, A., S. Verbridge, A. D. Stroock, C. Fischbach, and J. D. Varner. Multiscale models of breast cancer progression. *Ann. Biomed. Eng.* 40:2488–2500, 2012.
- ¹⁶Choi, T., M. R. Maurya, D. M. Tartakovsky, and S. Subramaniam. Stochastic operator-splitting method for reaction–diffusion systems. *J. Chem. Phys.* 137:184102, 2012.
- ¹⁷Christley, S., and G. An. Agent-Based Modeling in Translational Systems Biology. In: *Complex Systems and Computational Biology Approaches to Acute Inflammation SE—3*, edited by Y. Vodovotz, and G. An. New York, NY: Springer, 2013, pp. 29–49.
- ¹⁸Cilfone, N. A., C. R. Perry, D. E. Kirschner, and J. J. Linderman. Multi-scale modeling predicts a balance of tumor necrosis factor- α and interleukin-10 controls the granuloma environment during *Mycobacterium tuberculosis* infection. *PLoS ONE* 8:e68680, 2013.
- ¹⁹Costa, B. Spectral methods for partial differential equations. *Cubo - Revista de Matemática* 6:1–32, 2004.
- ²⁰Coveney, P. V., and P. W. Fowler. Modelling biological complexity: a physical scientist’s perspective. *J. R. Soc. Interface* 2:267–280, 2005.
- ²¹Csomós, P., I. Faragó, and Á. Havasi. Weighted sequential splittings and their analysis. *Comput. Math. Appl.* 50:1017–1031, 2005.
- ²²Dada, J. O., and P. Mendes. Multi-scale modelling and simulation in systems biology. *Integr. Biol. (Camb)* 3:86–96, 2011.
- ²³Daubechies, I. The wavelet transform, time-frequency localization and signal analysis. *IEEE Trans. Inf. Theory* 36:961–1005, 1990.
- ²⁴Deisboeck, T. S., Z. Wang, P. Macklin, and V. Cristini. Multiscale cancer modeling. *Annu. Rev. Biomed. Eng.* 13:127–155, 2011.
- ²⁵Duhamel, P., and M. Vetterli. Fast fourier transforms: a tutorial review and a state of the art. *Signal Process.* 19:259–299, 1990.
- ²⁶Fallahi-Sichani, M., M. El-Kebir, S. Marino, D. E. Kirschner, and J. J. Linderman. Multiscale computational modeling reveals a critical role for TNF- α receptor 1 dynamics in tuberculosis granuloma formation. *J. Immunol.* 186:3472–3483, 2011.
- ²⁷Fallahi-Sichani, M., J. L. Flynn, J. J. Linderman, and D. E. Kirschner. Differential risk of tuberculosis reactivation among anti-TNF therapies is due to drug binding kinetics and permeability. *J. Immunol.* 188:3169–3178, 2012.
- ²⁸Fallahi-Sichani, M., D. E. Kirschner, and J. J. Linderman. NF- κ B signaling dynamics play a key role in infection control in tuberculosis. *Front. Physiol.* 3:170, 2012.
- ²⁹Figueredo, G. P., T. V. Joshi, J. M. Osborne, H. M. Byrne, and M. R. Owen. On-lattice agent-based simulation of populations of cells within the open-source Chaste framework. *Interface Focus* 3:20120081, 2013.
- ³⁰Flynn, J. L., and J. Chan. Immunology of tuberculosis. *Annu. Rev. Immunol.* 19:93–129, 2001.
- ³¹Fornberg, B. *A practical guide to pseudospectral methods*. Cambridge: Cambridge University Press, 1996.
- ³²Frieboes, H. B., *et al.* Computer simulation of glioma growth and morphology. *Neuroimage* 37(Suppl 1):S59–S70, 2007.
- ³³Frigo, M., and S. G. Johnson. The Design and Implementation of FFTW3. *Proc. IEEE* 93:216–231, 2005.
- ³⁴Geiser, J., G. Tanoğlu, and N. Gücüyenen. Higher order operator splitting methods via Zassenhaus product formula: theory and applications. *Comput. Math. Appl.* 62:1994–2015, 2011.
- ³⁵Gong, C., J. J. Linderman, and D. Kirschner. Harnessing the heterogeneity of T cell differentiation fate to fine-tune generation of effector and memory T cells. *Front. Immunol.* 5:1–15, 2014.
- ³⁶Gong, C., J. T. Mattila, M. Miller, J. L. Flynn, J. J. Linderman, and D. Kirschner. Predicting lymph node output efficiency using systems biology. *J. Theor. Biol.* 335C:169–184, 2013.
- ³⁷Gottlieb, D., and C.-W. Shu. On the Gibbs phenomenon and its resolution. *SIAM Rev.* 39:644–668, 1997.
- ³⁸Guo, Z., P. M. A. Sloot, and J. C. Tay. A hybrid agent-based approach for modeling microbiological systems. *J. Theor. Biol.* 255:163–175, 2008.
- ³⁹Hedengren, J. D., and T. F. Edgar. Order reduction of large scale DAE models. *Comput. Chem. Eng.* 29:2069–2077, 2005.
- ⁴⁰Hedengren, J. D., and T. F. Edgar. *In situ* adaptive tabulation for real-time control. *Ind. Eng. Chem. Res.* 44:2716–2724, 2005.
- ⁴¹Heidlauf, T., and O. Röhrle. Modeling the chemo-electromechanical behavior of skeletal muscle using the parallel open-source software library OpenCMISS. *Comput. Math. Methods Med.* 2013:517287, 2013.
- ⁴²Holcombe, M., *et al.* Modelling complex biological systems using an agent-based approach. *Integr. Biol. (Camb)* 4:53–64, 2012.
- ⁴³Hou, T. Y., and R. Li. Computing nearly singular solutions using pseudo-spectral methods. *J. Comput. Phys.* 226:379–397, 2007.
- ⁴⁴Hunt, C. A., R. C. Kennedy, S. H. J. Kim, and G. E. P. Ropella. Agent-based modeling: a systematic assessment of use cases and requirements for enhancing pharmaceutical research and development productivity. *Wiley Interdiscip. Rev. Syst. Biol. Med.* 5:461–480, 2013.
- ⁴⁵Karlsen, K. H., K.-A. Lie, J. Natvig, H. Nordhaug, and H. Dahle. Operator splitting methods for systems of convec-

- tion–diffusion equations: nonlinear error mechanisms and correction strategies. *J. Comput. Phys.* 173:636–663, 2001.
- ⁴⁶Kaul, H., Z. Cui, and Y. Ventikos. A multi-paradigm modeling framework to simulate dynamic reciprocity in a bioreactor. *PLoS ONE* 8:e59671, 2013.
- ⁴⁷Kim, M., R. J. Gillies, and K. A. Rejniak. Current advances in mathematical modeling of anti-cancer drug penetration into tumor tissues. *Front. Oncol.* 3:278, 2013.
- ⁴⁸Kirschner, D. E., S. T. Chang, T. W. Riggs, N. Perry, and J. J. Linderman. Toward a multiscale model of antigen presentation in immunity. *Immunol. Rev.* 216:93–118, 2007.
- ⁴⁹Kirschner, D. E., C. A. Hunt, S. Marino, M. Fallahi-Sichani, and J. J. Linderman. Tuneable resolution as a systems biology approach for multi-scale, multi-compartment computational models. *Wiley Interdiscip. Rev. Syst. Biol. Med.* 6:289–309, 2014.
- ⁵⁰Krinner, A., I. Roeder, M. Loeffler, and M. Scholz. Merging concepts—coupling an agent-based model of hematopoietic stem cells with an ODE model of granulopoiesis. *BMC Syst. Biol.* 7:117, 2013.
- ⁵¹Lauffenburger, D. A., and J. J. Linderman. *Receptors: Models For Binding, Trafficking, and Signaling*. New York: Oxford University Press, 1993.
- ⁵²LeVeque, R. J. *Finite Difference Methods for Ordinary and Partial Differential Equations*. Society for Industrial and Applied Mathematics, 2007.
- ⁵³Linderman, J. J., and D. E. Kirschner. *In silico* models of *M. tuberculosis* infection provide a route to new therapies. *Drug Discov. Today Dis. Model.* 1–5, 2014.
- ⁵⁴Lucas, T. A. Operator splitting for an immunology model using reaction–diffusion equations with stochastic source terms. *SIAM J. Numer. Anal.* 46:3113–3135, 2008.
- ⁵⁵Marino, S., M. El-Kebir, and D. Kirschner. A hybrid multi-compartment model of granuloma formation and T cell priming in tuberculosis. *J. Theor. Biol. Elsevier* 280:50–62, 2011.
- ⁵⁶Marino, S., I. B. Hogue, C. J. Ray, and D. E. Kirschner. A methodology for performing global uncertainty and sensitivity analysis in systems biology. *J. Theor. Biol.* 254:178–196, 2008.
- ⁵⁷Marino, S., J. J. Linderman, and D. E. Kirschner. A multifaceted approach to modeling the immune response in tuberculosis. *Wiley Interdiscip. Rev. Syst. Biol. Med.* 3:479–489, 2011.
- ⁵⁸Materi, W., and D. S. Wishart. Computational systems biology in drug discovery and development: methods and applications. *Drug Discov. Today* 12:295–303, 2007.
- ⁵⁹Mitha, F., T. A. Lucas, F. Feng, T. B. Kepler, and C. Chan. The multiscale systems immunology project: software for cell-based immunological simulation. *Source Code Biol. Med.* 3:6, 2008.
- ⁶⁰Mugler, D. H., and R. A. Scott. Fast fourier transform method for partial differential equations, case study: the 2-D diffusion equation. *Comput. Math. Appl.* 16:221–228, 1988.
- ⁶¹Palsson, S., *et al.* The development of a fully-integrated immune response model (FIRM) simulator of the immune response through integration of multiple subset models. *BMC Syst. Biol.* 7:95, 2013.
- ⁶²Peaceman, D. W., and H. H. Rachford, Jr. The numerical solution of parabolic and elliptic differential equations. *J. Soc. Ind. Appl. Math.* 3:28–41, 1955.
- ⁶³Petersen, B. K., G. E. Ropella, and C. A. Hunt. Toward modular biological models: defining analog modules based on referent physiological mechanisms. *BMC Syst. Biol.* 8:95, 2014.
- ⁶⁴Pienaar, E., *et al.* A computational tool integrating host immunity with antibiotic dynamics to study tuberculosis treatment. *J. Theor. Biol.* 2014 (in Press).
- ⁶⁵Pope, S. B. Computationally efficient implementation of combustion chemistry using *in situ* adaptive tabulation. *Combust. Theory Model.* 1:41–63, 1997.
- ⁶⁶Press, W. H. *Numerical recipes in C++: the art of scientific computing* (2nd ed.). Cambridge, UK: Cambridge University Press, 2002.
- ⁶⁷Qutub, A. A., F. Mac Gabhann, E. D. Karagiannis, P. Vempati, and A. S. Popel. Multiscale models of angiogenesis. *IEEE Eng. Med. Biol. Mag.* 28:14–31, 2009.
- ⁶⁸Qutub, A. A., and A. S. Popel. Elongation, proliferation & migration differentiate endothelial cell phenotypes and determine capillary sprouting. *BMC Syst. Biol.* 3:13, 2009.
- ⁶⁹Rao, S., A. van der Schaft, K. van Eunen, B. M. Bakker, and B. Jayawardhana. A model reduction method for biochemical reaction networks. *BMC Syst. Biol.* 8:52, 2014.
- ⁷⁰Rapin, N., O. Lund, M. Bernaschi, and F. Castiglione. Computational immunology meets bioinformatics: the use of prediction tools for molecular binding in the simulation of the immune system. *PLoS ONE* 5:e9862, 2010.
- ⁷¹Ray, J. C. J., J. L. Flynn, and D. E. Kirschner. Synergy between individual TNF-dependent functions determines granuloma performance for controlling *Mycobacterium tuberculosis* infection. *J. Immunol.* 182:3706–3717, 2009.
- ⁷²Riley, K. F., M. P. Hobson, and S. J. Bence. *Mathematical Methods for Physics and Engineering: A Comprehensive Guide*. Cambridge: Cambridge University Press, 2002.
- ⁷³Santoni, D., M. Pedicini, and F. Castiglione. Implementation of a regulatory gene network to simulate the TH1/2 differentiation in an agent-based model of hypersensitivity reactions. *Bioinformatics* 24:1374–1380, 2008.
- ⁷⁴Segovia-Juarez, J. L., S. Ganguli, and D. Kirschner. Identifying control mechanisms of granuloma formation during *M. tuberculosis* infection using an agent-based model. *J. Theor. Biol.* 231:357–376, 2004.
- ⁷⁵Singer, M., S. Pope, and H. Najm. Modeling unsteady reacting flow with operator splitting and ISAT. *Combust. Flame* 147:150–162, 2006.
- ⁷⁶Sloot, P. M. A., and A. G. Hoekstra. Multi-scale modelling in computational biomedicine. *Brief. Bioinform.* 11:142–152, 2010.
- ⁷⁷Southern, J., *et al.* Multi-scale computational modelling in biology and physiology. *Prog. Biophys. Mol. Biol.* 96:60–89, 2008.
- ⁷⁸Stefanini, M. O., F. T. H. Wu, F. Mac Gabhann, and A. S. Popel. The presence of VEGF receptors on the luminal surface of endothelial cells affects VEGF distribution and VEGF signaling. *PLoS Comput. Biol.* 5:e1000622, 2009.
- ⁷⁹Stern, J. R., S. Christley, O. Zaborina, J. C. Alverdy, and G. An. Integration of TGF- β - and EGFR-based signaling pathways using an agent-based model of epithelial restitution. *Wound Repair Regen.* 20:862–871, 2012.
- ⁸⁰Strang, G. On the construction and comparison of difference schemes. *SIAM J. Numer. Anal.* 5:506–517, 1968.
- ⁸¹Sun, T., S. Adra, R. Smallwood, M. Holcombe, and S. MacNeil. Exploring hypotheses of the actions of TGF-beta1 in epidermal wound healing using a 3D computational multiscale model of the human epidermis. *PLoS ONE* 4:e8515, 2009.
- ⁸²Sundnes, J., G. T. Lines, and A. Tveito. An operator splitting method for solving the bidomain equations

- coupled to a volume conductor model for the torso. *Math. Biosci.* 194:233–248, 2005.
- ⁸³Swat, M. H., G. L. Thomas, J. M. Belmonte, A. Shirinifard, D. Hmeljak, and J. A. Glazier. Multi-scale modeling of tissues using CompuCell 3D. *Methods Cell Biol.* 110:325–366, 2012.
- ⁸⁴Tay, S., J. J. Hughey, T. K. Lee, T. Lipniacki, S. R. Quake, and M. W. Covert. Single-cell NF-kappaB dynamics reveal digital activation and analogue information processing. *Nature* 466:267–271, 2010.
- ⁸⁵Trefethen, L. N. *Finite Difference and Spectral Methods for Ordinary and Partial Differential Equations*. Unpublished Text, 1996.
- ⁸⁶Walker, D. C., and J. Southgate. The virtual cell—a candidate co-ordinator for “middle-out” modelling of biological systems. *Brief. Bioinform.* 10:450–461, 2009.
- ⁸⁷Walpole, J., J. A. Papin, and S. M. Peirce. Multiscale computational models of complex biological systems. *Annu. Rev. Biomed. Eng.* 15:137–154, 2013.
- ⁸⁸Wang, Z., V. Bordas, J. Sagotsky, and T. S. Deisboeck. Identifying therapeutic targets in a combined EGFR-TGF β R signalling cascade using a multiscale agent-based cancer model. *Math. Med. Biol.* 29:95–108, 2012.
- ⁸⁹Wang, Z., J. D. Butner, R. Kerketta, V. Cristini, and T. S. Deisboeck. Simulating cancer growth with multiscale agent-based modeling. *Semin. Cancer Biol.* 1–9, 2014. doi: [10.1016/j.semcancer.2014.04.001](https://doi.org/10.1016/j.semcancer.2014.04.001).
- ⁹⁰Wang, J., *et al.* Multi-scale agent-based modeling on melanoma and its related angiogenesis analysis. *Theor. Biol. Med. Model.* 10:41, 2013.
- ⁹¹Wise, S., J. Kim, and J. Lowengrub. Solving the regularized, strongly anisotropic Cahn–Hilliard equation by an adaptive nonlinear multigrid method. *J. Comput. Phys.* 226:414–446, 2007.
- ⁹²Wise, S. M., J. S. Lowengrub, and V. Cristini. An adaptive multigrid algorithm for simulating solid tumor growth using mixture models. *Math. Comput. Model.* 53:1–20, 2011.
- ⁹³Wolff, K., C. Barrett-Freeman, M. R. Evans, A. B. Goryachev, and D. Marenduzzo. Modelling the effect of myosin X motors on filopodia growth. *Phys. Biol.* 11:016005, 2014.
- ⁹⁴Yoshida, H. Construction of higher order symplectic integrators. *Phys. Lett. A* 150:262–268, 1990.
- ⁹⁵Zhang, L., *et al.* Developing a multiscale, multi-resolution agent-based brain tumor model by graphics processing units. *Theor. Biol. Med. Model.* 8:46, 2011.
- ⁹⁶Zingg, D. W., and T. T. Chisholm. Runge-Kutta methods for linear ordinary differential equations. *Appl. Numer. Math.* 31:227–238, 1999.